Scanning Microscopy, Vol. 9, No. 2, 1995 (Pages 429-442) 0891-7035/95$5.00+.25
Scanning Microscopy International, Chicago (AMF O'Hare), IL 60666 USA

MAMMALIAN ENAMEL PRISM PATTERNS AND ENAMEL DEPOSITION RATES

Elizabeth R. Dumont*

Department of Anthropology, Social and Behavioral Sciences Building
State University of New York at Stony Brook, Stony Brook, New York 11794

(Received for publication August 9, 1994 and in revised form June 9, 1995)

Abstract

Enamel prism patterns and enamel deposition rates were compared for specimens representing six mammalian orders. Enamel samples were characterized by either pattern 1 or pattern 3 prisms. Each prism pattern category contained prisms from at least two mammalian orders. Enamel deposition rate was estimated for each sample by measuring prism cross striation repeat intervals. Statistical analysis of cross striation repeat intervals illustrates significant differences in deposition rate between prism patterns 1 and 3. No statistically significant differences were found in deposition rate between the higher-level taxa represented within each prism pattern category. That enamel deposition rate is not taxon-specific reinforces the close association between deposition rate and prism morphology. In accord with previous studies, pattern 1 enamel is deposited more slowly than is pattern 3 enamel. Correlation analyses illustrated a lack of association between enamel deposition rate and body mass, tooth size, and estimated ameloblast size. Evidence that enamel deposition rate is associated with enamel prism morphology, coupled with evidence that deposition rate is not correlated with size parameters, points to developmental homology (i.e., homogeneous deposition rate) within each prism pattern.

Key Words: Enamel, prism patterns, deposition rates, cross striation repeat intervals, evolution.

*Address for correspondence:
E.R. Dumont
Department of Neurobiology,
University of Pittsburgh School of Medicine,
818A Scaife Hall,
Pittsburgh, PA 15261.
Telephone number: (412) 648-9788
FAX number: (412) 648-1441

Introduction

Mammalian dental enamel is mainly composed of submicroscopic hydroxyapatite crystallites. Discontinuities surrounding bundles of similarly oriented crystallites define enamel prisms, which extend from the dentine core of a tooth toward the outer surface of the enamel. Enamel prism patterns are divided into three basic categories based on their prism shape and packing patterns as seen in tangential sections of mature enamel (Fig. 1) (Korvenkontio, 1934-1935; Boyde, 1964, 1967, 1971). Prism pattern 1 consists of prisms with complete boundaries that are arranged in offset horizontal rows with respect to the apico-cervical axis of the tooth. In pattern 2, prisms are arc-shaped and arranged in offset vertical rows separated by a distinct inter-row sheet, while arc-shaped prisms arranged in offset horizontal rows constitute pattern 3.

A growing body of evidence suggests that enamel prism patterns are correlated with variations in enamel deposition rates (Moss, 1969; Osborn, 1970; Martin, 1983, 1985; Martin and Boyde, 1984; Fortelius, 1985). The consistency of this relationship has implications concerning the value of prism patterns in evolutionary studies. If prism patterns are rate dependent, changes in secretory rate could be the cause of apparent divergence, convergence, and parallelism in enamel prism pattern morphology. Alternatively, if prism patterns are not rate dependent, then variation in rate within prism pattern categories may serve to characterize specific mammalian lineages.

The goal of this study is to test two hypotheses concerning the relationship between enamel prism pattern morphology and enamel deposition rate. The first hypothesis states that enamel prism pattern morphology is associated with specific enamel deposition rates. To test this hypothesis, enamel deposition rates were compared between prism pattern categories that were each represented by several different mammalian orders. The combination of several orders in each category ensured that comparisons would reflect differences among prism patterns rather than differences among taxonomic groups.

The second hypothesis states that, within a prism pattern category, different taxa are characterized by taxon-specific enamel deposition rates. This hypothesis was addressed through comparisons of enamel deposition rates between distantly related taxa within each of two prism pattern categories. Finally, associations between deposition rate and body mass, tooth size, and ameloblast size were assessed using correlation analyses.

Materials and Methods

Taxonomic sample

Taxa were selected based on a priori expectations of prism packing patterns that were drawn from the literature. The living scandentian *Tupaia glis* and the erinaceids *Atelerix albiventris* and *Erinaceus europaeus* were selected to represent pattern 1 taxa (Boyde, 1964; Silness and Gustavsen, 1969; Shellis and Poole, 1977; Shellis, 1984a). Recent human (*Homo sapiens*), dermopteran (*Cynocephalus variegatus*), and chiropteran (*Balantiopteryx plicata*, *Rhinopoma hardwickei*, and *Taphozous mauritianus*) enamel was selected to represent pattern 3 taxa, as was enamel from the fossil family Microsyopidae (*Microsyops* sp.) (Martin, 1983; Lester and Hand, 1987; Lester *et al.*, 1988; Martin *et al.*, 1988; Dumont, 1993). Single specimens of *Galagoides alleni*, *G. demidovii*, and the fossil primate *Notharctus* sp. were also anticipated to express prism pattern 3 (Dumont, 1993). The living cercopithecid primates *Macaca fascicularis*, *Cercocebus torquatus* and *Cercocebus albigena* were chosen to represent prism pattern 2, which has been reported to occur within this primate family (Boyde and Martin, 1984a, 1984b, 1987; Martin *et al.*, 1988).

Microscopic techniques

Specimens were embedded in polymethylmethacrylate and sectioned longitudinally through the protoconid and metaconid tips. The sectioned specimens were then polished with successively finer diamond pastes (6 μm, 4 μm, 1 μm, and 0.25 μm). Between polishing treatments, specimens were cleaned with a detergent (Mr. Clean®) and rinsed with distilled water for approximately five minutes to insure that all grit and oils were removed. When polishing was complete, specimens were cleaned again, allowed to air dry overnight, and mounted with Duco Cement® on scanning electron microscope (SEM) stubs. Following an overnight curing period, specimens were etched with 0.5% H_3PO_4 for seven to 20 seconds; smaller recent specimens required less etching than did larger fossil specimens. The chemical reaction was stopped by immediately quenching the specimens, with agitation, in a distilled water bath for one minute. Specimens were then rinsed under running tap water for one minute and immediately rinsed again in fresh distilled water for 30 seconds. Following another overnight drying period, specimens were sputter-coated with silver for 60 to 70 seconds in ten second bursts in final preparation for SEM viewing.

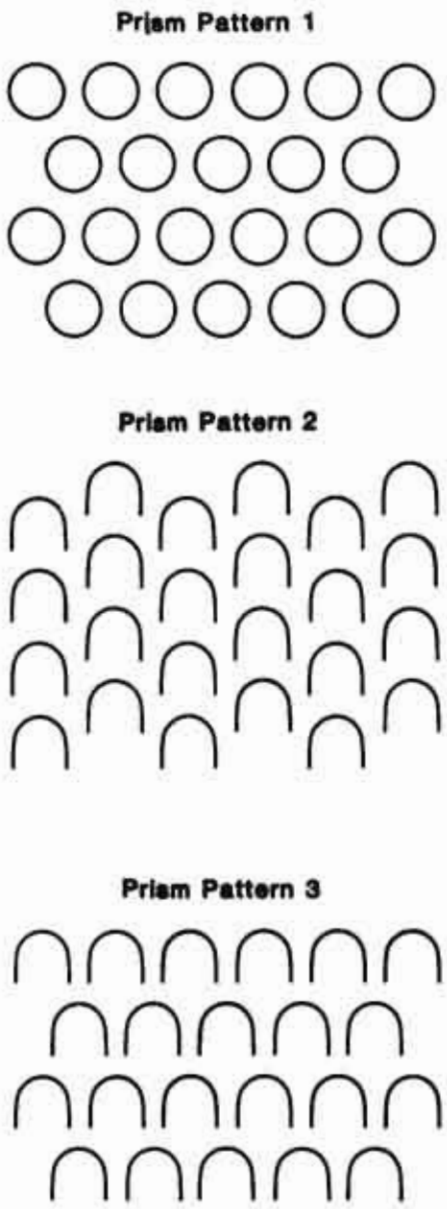

Figure 1. Diagram illustrating enamel prism patterns 1, 2 and 3. Each pattern exhibits a unique combination of enamel prism shape and spatial organization.

All microscopy was accomplished using an AMRAY® model 1810D SEM equipped with a solid state backscattered electron detector. Accelerating voltages (kV) ranging from 25 to 30 were used in conjunction with a working distance of 9 to 12 mm, a condenser lens setting between 2.5 and 4.0, and either

Table 1. Summary by specimen of methods used to couple prism pattern and cross striation repeat intervals. Taxon, specimen number (Number), number of micrographs (Nmicro), total number of measured cross striations (Nstriae), and sampled tooth position (Tooth) is listed for each specimen. Methods used to link prism pattern and cross striation listed in order of decreasing reliability are: direct evidence of prism pattern on the same micrograph (Direct), prism pattern determined by confocal microscopy of the same specimen (TSM), and prism pattern determined by confocal microscopy of other specimens of the same species (TSother, (N) = sample size).

Taxon	Number	Nmicro	Nstriae	Direct	TSM	TSother (N)	Tooth
PATTERN 1							
Atelerix albiventris	FSM 20551	3	30	x			right M^1
	FSM 20552	3	50	x			right M_1
	FSM 20553	4	55	x			right M_1
Erinaceus europaeus	TT 49630	3	11	x			right M_1
	TT 49631	1	14	x			right M_1
Tupaia glis	SUSB (1)*	2	14			x (3)	right M_1
	SUSB (2)*	3	40	x			right M_1
	SUSB (3)*	1	7			x (3)	right M_1
PATTERN 3							
Balantiopteryx plicata	TT 38121	4	56			x (4)	right M_1
	TT 38122	3	60		x		right M_1
	TT 38123	1	4		x		right M_1
	TT 38128	2	27		x		right M_1
Cynocephalus variegatus	DZUM 100	2	21			x (5)	right M_1
	FMNH 56505	3	74			x (5)	right M_1
	FMNH 56524	1	9			x (5)	right M_1
	RVNH 15822	1	2			x (5)	right M_1
Homo sapiens	SUSB (1)*	3	35	x			right M_1
	SUSB (2)*	3	75	x			left M_1
	SUSB (3)*	2	47			x	right M_1
	SUSB (4)*	1	22			x	right M_1
	SUSB (5)*	3	75	x			right M_1
Microsyops sp.†	CM (1)*	1	4	x			right M_1
	CM (3)*	1	2	x			M_x frag.
Rhinopoma hardwickei	TT 40638	2	22		x		right M_1
	TT 40640	1	12	x			right M_1
Taphozous mauritianus	CM 85237	3	72			x (11)	right M_1
	CM 85241	3	65			x (11)	right M_1
MIXED PATTERNS 2 AND 3							
Cercocebus albigena	SUSB 85-17	5	105			x (1)	right M_3
	SUSB 85-7	1	5			x (1)	right M_3
Cercocebus torquatus	ANSP 3072	1	18			x (1)	right M_1
	ANSP 12645	4	97			x (1)	right M_1
	ANSP 11840	3	75			x (1)	right M_1
Macaca fasicularis	(1)*	1	10			x (1)	right M_1
	(2)*	3	45			x (1)	right M_1
SINGLE SPECIMENS ILLUSTRATING PATTERN 3							
Galagoides demidovii	SUSB PGa1	2	21			x (2)	right M_1
Notharctus sp.†	CM*	1	6	x			M_x frag.
PRISM PATTERN NOT DETERMINED							
Galagoides alleni	CM 3898	3	66				right M_1

* = uncataloged specimens; † = fossil taxon.

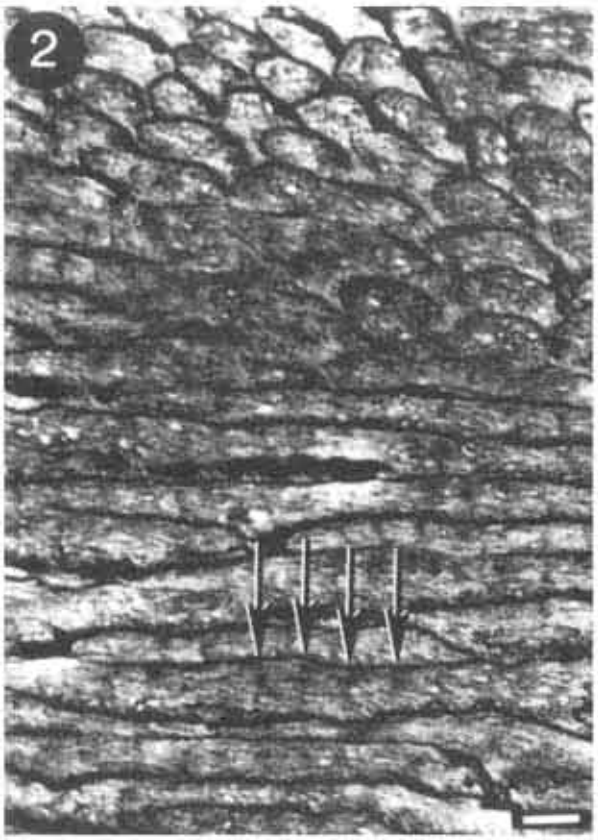

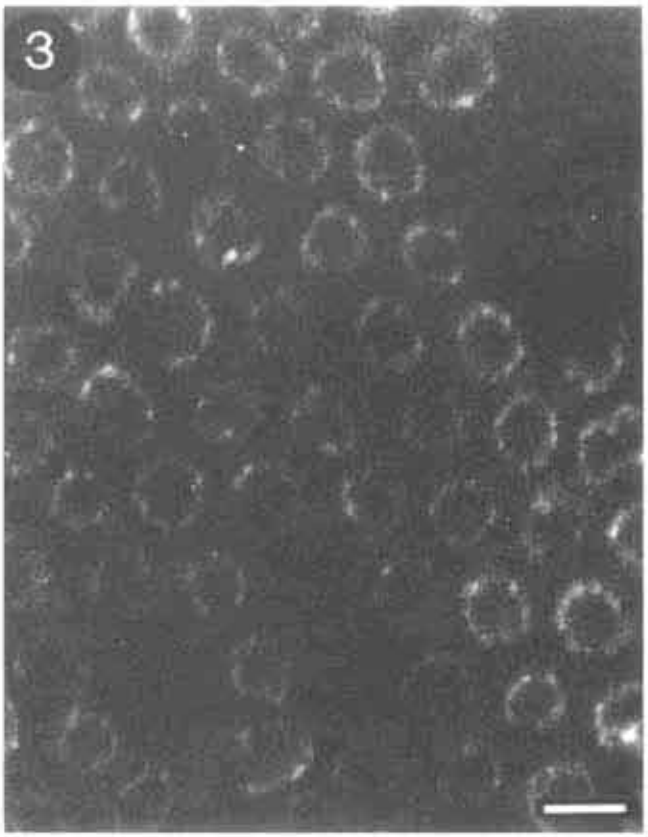

Figure 2. BSE image of longitudinally sectioned human enamel. Pattern 3 prisms are visible within the upper portion of the micrograph. Arrows point to a series of cross striations along a single prism. Bar = 10 μm.

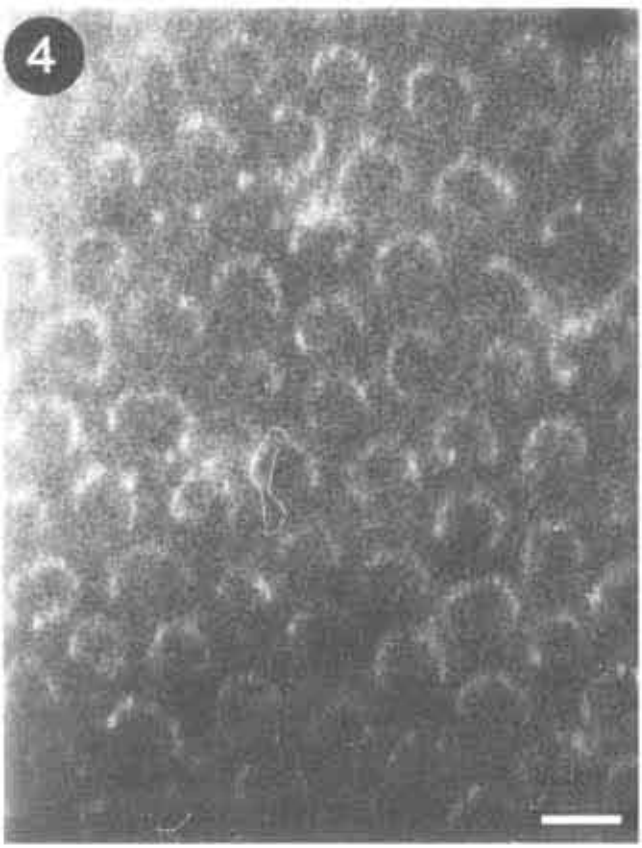

Figure 3. Confocal image of *Tupaia glis* (SUSB) enamel taken at a depth of 25 μm below the buccal surface of the right M^1 hypoconid. Bar = 5 μm.

Figure 4. Confocal image of *Cynocephalus variegatus* enamel (RVNH 14516) taken at a depth of 25 μm below the buccal surface of the right M^1 protoconid. Bar = 5 μm.

---

a 200 μm or 300 μm aperture. This combination of settings was found through trial and error to produce the highest resolution and maximum contrast, while providing an acceptable signal to noise ratio.

Association between cross-striations and prism pattern

Enamel for analysis of enamel deposition rates was sampled from the central portion of the enamel thickness of 38 molar teeth, 77 areas from either the mid-thickness of the buccal aspect of the protoconid or the lingual aspect of the metaconid and 7 areas from the trigonid basin.

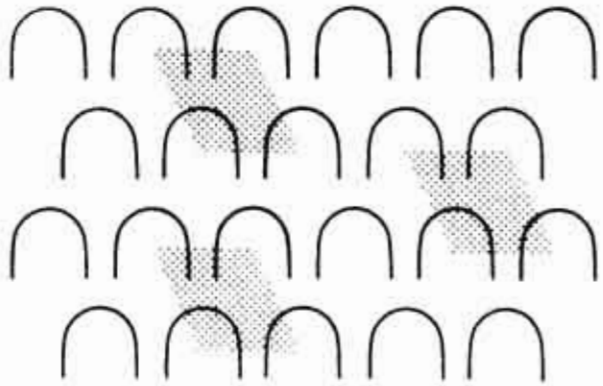

Figure 5. Using formulas developed by Fosse (1968a), the estimated area of a single ameloblast is calculated as the area of a parallelogram drawn between the centers of adjacent prisms. In this diagram, three parallelograms are represented as shaded areas.

Because enamel prism pattern morphology can vary within a tooth, it was important to associate measurements of enamel prism cross striations with cross-sectional prism morphology as directly as possible. Table 1 presents a summary of the sampled specimens and the methods used to couple prism pattern categories and photomicrographs of longitudinally sectioned prisms.

For 35% of the specimens, prism pattern assignments were confirmed by viewing cross-sectioned prisms exposed on longitudinal sections in regions adjacent to those in which prism cross striations were present (Fig. 2). For a few specimens, prism pattern was confirmed by examining tangential sections of subsurface enamel using confocal microscopy. Prism pattern could not be resolved for the single specimen of *Galagoides alleni*. Evidence for prism pattern assignments summarizing the remaining 50% of the specimens were based on the prism pattern found on tangential sections of homologous teeth from conspecific individuals; these sections were viewed using confocal microscopy (Figs. 3 and 4).

Measurement methods

Cross striations and micron scales on enlarged micrographs were traced and measured on acetate overlays. Distances between the centers of adjacent cross striation repeat intervals were measured parallel to prism long axes to the nearest 0.1 mm using dial calipers. Sampling of cross-striations on the periphery of micrographs was avoided whenever possible. The orientation of cross striations to larger incremental features was not investigated. Up to 25 cross striation repeat intervals were measured from each micrograph. Each cross striation was numbered for future reference. All measurements were brought to the same scale prior to statistical comparisons.

Statistical analysis

The two hypotheses concerning prism pattern and cross striation repeat intervals were addressed separately using single classification analysis of variance (ANOVA). This method was determined to be the most appropriate method of comparison, as the data are both normal and homoscedastic (Sokal and Rohlf, 1981). In analyzing whether cross striation repeat intervals are significantly different between pattern 1 and pattern 3 enamel, specimen means of cross striation repeat intervals from pattern 1 taxa (*Erinaceus*, *Atelerix*, and *Tupaia*) were compared to specimen means from pattern 3 taxa (*Taphozous*, *Balantiopteryx*, *Rhinopoma*, *Homo*, *Cynocephalus*, and *Microsyops*).

In order to test the second hypothesis, that significant variation in cross striation repeat intervals exists among taxa within prism pattern categories, scandentians were compared to erinaceids for the pattern 1 case, while chiropteran, *Cynocephalus*, *Homo*, and *Microsyops* specimens were compared simultaneously for the pattern 3 case. Again, specimen means were used to represent variation that occurs among individuals within each higher-level group.

Associations between cross striation repeat interval and body mass, tooth area (mesiodistal length x buccolingual breadth), and estimated ameloblast area were assessed using correlation analyses. Estimated ameloblast area was calculated using confocal images of tangentially sectioned enamel prisms from molar teeth of conspecific individuals. Following the method developed by Fosse (1968a) and used by many subsequent workers (Carlson and Krause, 1985; Fosse *et al.*, 1985; Grine *et al.*, 1986, 1987; Krause and Carlson, 1986), estimated ameloblast area was calculated as the area of a parallelogram drawn between the centers of four adjacent prisms (Fig. 5).

All variables were transformed to a linear scale by taking roots and logged to reduce the effects of magnitude on the correlation coefficient (Smith, 1984). Because the transformed data were normal and displayed homogeneous variances, the parametric Product-Moment correlation test was used to analyze each set of paired data (Sokal and Rohlf, 1981). These analyses do not rely on prism pattern assignments and data from the three sampled cercopithecid primates were included. Samples from single specimens (i.e., *Galagoides demidovii*, *Galagoides alleni* and *Notharctus* sp.) were also incorporated into the analysis to provide a larger sample size. Due to missing data, one or more taxa were omitted from each analysis; *Homo* was excluded from analyses of tooth area; *Galagoides alleni* and the

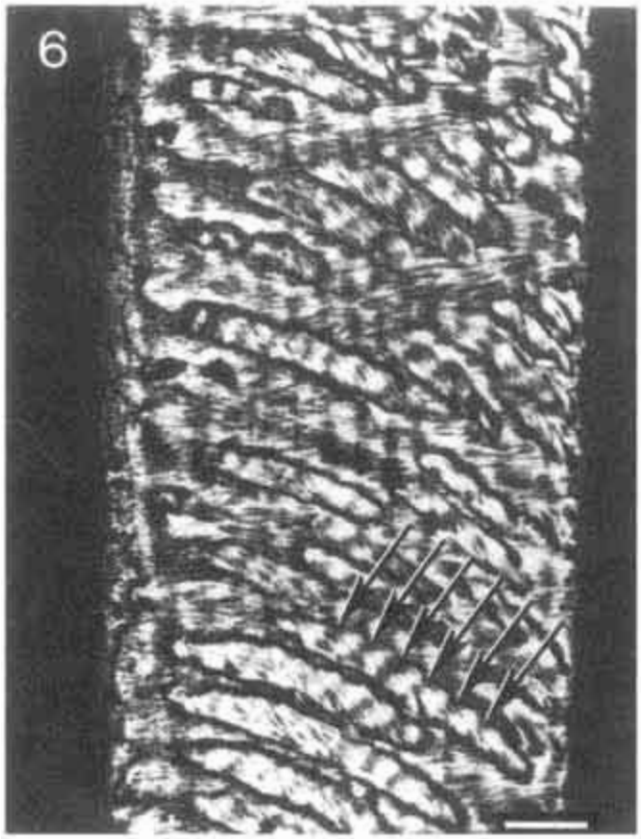
6

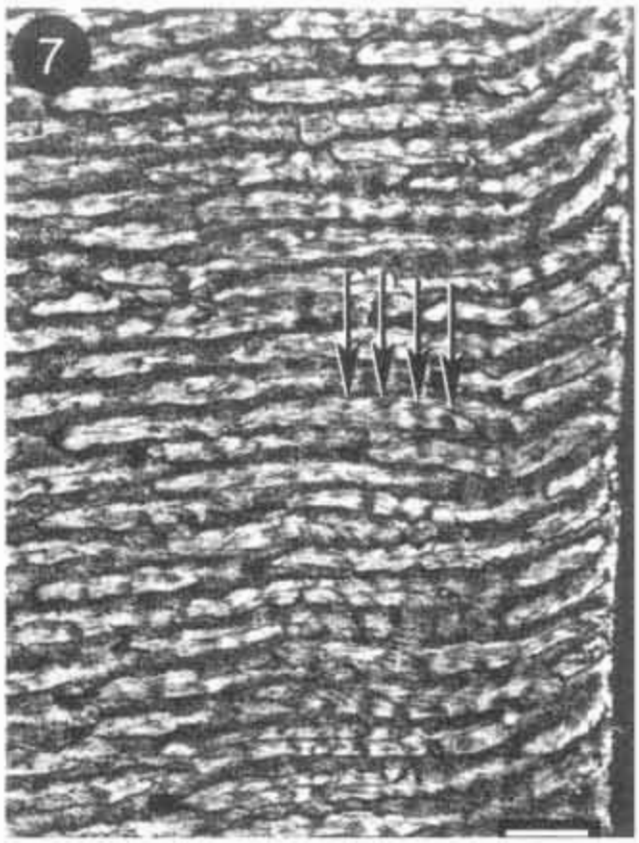
7

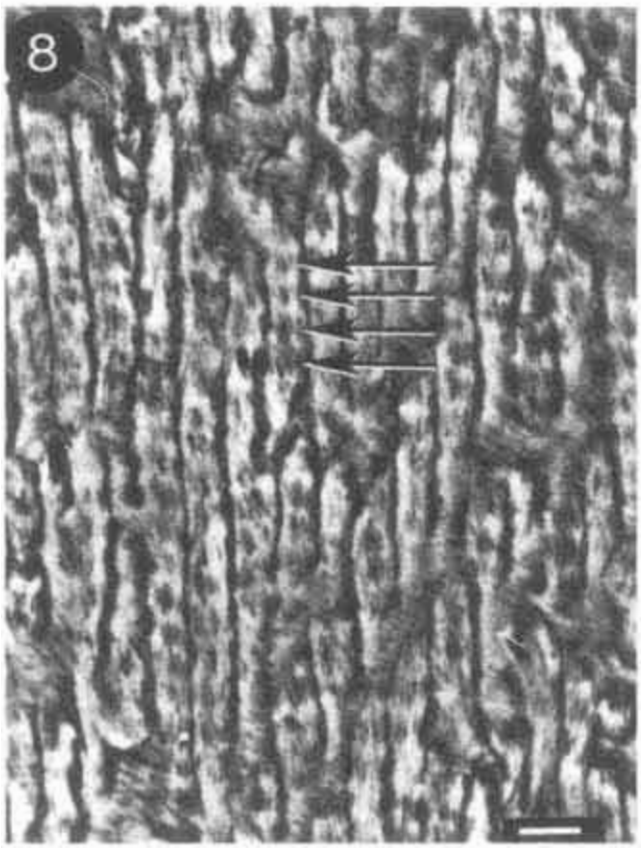
8

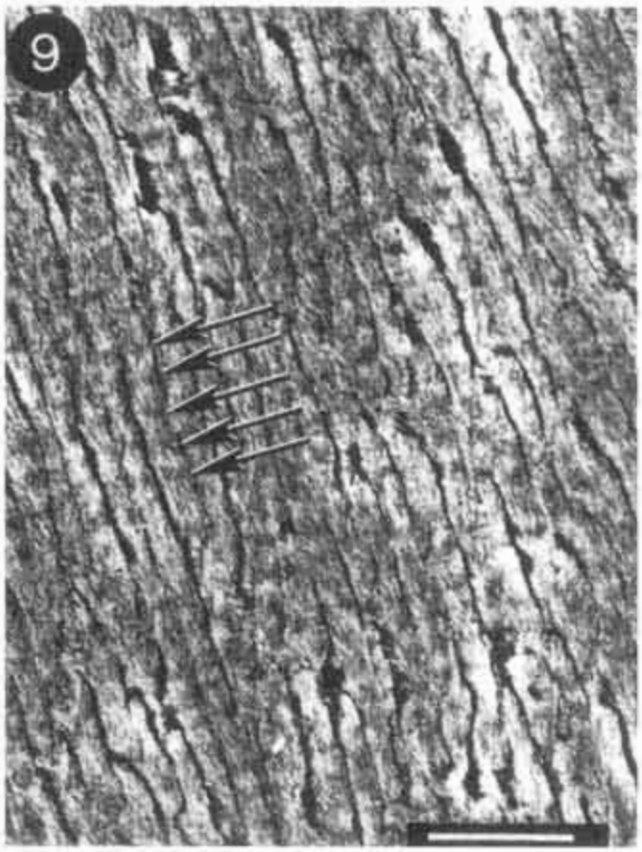
9

Figures 6-9 are on the facing page.

Figure 6. BSE image of longitudinally sectioned prisms in *Taphozous mauritianus* (CM 85237) enamel. Arrows point to a series of cross striations along a single prism. Bar = 10 μm.

Figure 7. BSE image of longitudinally sectioned prisms in *Galagoides alleni* (CM 3898) enamel. Arrows point to a series of cross striations along a single prism. Bar = 10 μm.

Figure 8. BSE image of longitudinally sectioned prisms in *Homo sapiens* (SUSB, not cataloged) enamel. Arrows point to a series of cross striations along a single prism. Bar = 10 μm.

Figure 9. BSE image of longitudinally sectioned prisms in *Cercocebus torquatus* (ANSP 12645) enamel. Arrows point to a series of cross striations along a single prism. Bar = 10 μm.

---

cercopithecid primates were excluded from analyses of ameloblast area; and fossil taxa were excluded from analyses involving body mass.

Results

When viewed using backscattering electron microscopy (BSE), cross striations appear as alternating light and dark bands (Figs. 6-9). With the exceptions of *Homo sapiens* and *Erinaceus europaeus*, prisms within these taxa exhibit relatively straight courses from the enamel-dentine junction to the outer enamel surface (i.e., there was no evidence of prism decussation zones).

Comparisons of cross striation repeat intervals between individuals of the same species using single classification ANOVA illustrated that in 8 of 9 cases, conspecific individuals differ significantly from one another. This indicates that cross striation repeat intervals from a single specimen are unlikely to represent the range of cross striation values for an entire species. Therefore, species represented by only one individual (e.g., *Notharctus* sp., *Galagoides demidovii*, and *Galagoides alleni*) were deleted from comparisons of cross striation repeat intervals between prism pattern categories. In addition, it was not possible to confirm the sole presence of pattern 2 prisms in any of the species that were expected to exhibit the prism pattern. Therefore, the prism pattern 2 category was deleted from further analyses.

Table 2 presents summary statistics for each sampled taxon, as well as results of statistical comparisons of prism cross striation repeat intervals within and between prism pattern 1 and 3 categories. Taxa characterized by prism pattern 1 exhibit more narrowly spaced cross striations than do taxa that are characterized by prism pattern 3. Cross striation repeat intervals are significantly different between the two prism pattern categories ($p < .01$). Within each pattern category, values representing species were very similar. Comparisons between species within each prism pattern category illustrated that there were no significant differences between representatives of different mammalian orders.

Table 3 presents cross striation repeat intervals, body mass, tooth area, and ameloblast area data for each species, as well as correlation coefficients summarizing associations between cross striation repeat interval and each of the size variables. The correlation coefficients for body mass and tooth area analyses are of similar magnitude at $r = 0.23$ and $r = 0.30$, respectively. The correlation between cross striation repeat intervals and ameloblast area is slightly lower at $r = 0.16$. None of these correlation coefficients differ significantly from zero.

Discussion

In his original description of prism patterns, Boyde (1964) described several subdivisions of the pattern 2 and 3 categories that were subsequently elaborated by Gantt (1982, 1983). Although many taxa within this study exhibit pattern 3 enamel, it proved difficult to assign pattern 3 prisms to any one subdivision because of minor variations in prism distribution within even limited areas of individual teeth. Rather than using ill-fitting subcategories, all taxa with unambiguous prism patterns were categorized as either prism pattern 1 or 3. Although Shellis (1984a) described dermopteran enamel as exhibiting pattern 2 prisms, no evidence of consistent vertical prism stacking or inter-row sheets was encountered in this analysis and dermopterans were retained in the prism pattern 3 category.

It proved impossible to verify the exclusive presence of pattern 2 prisms in the cercopithecoid primates. The specimens used in this study exhibited arc-shaped prisms that were arranged in both pattern 3 and pattern 2 spatial distributions. No clear indications of inter-row sheets were seen in any specimens. A similarly mixed distribution of arc-shaped prisms among cercopithecoid primates have been reported by several other workers (Shellis and Poole, 1977; Shellis, 1984a, 1984b; Grine *et al.*, 1985; Martin *et al.*, 1988), adding support to the current finding of mixed patterns 2 and 3 in these taxa.

Within any individual tooth, enamel prism pattern morphology exhibits variations attributable to changes in ameloblast (enamel matrix secreting cell) Tomes' process configuration during enamel deposition; a layer of aprismatic enamel resides at both the enamel-dentine

Table 2. Summary statistics for each sampled taxon and results of statistical comparisons of cross striation repeat intervals within and between prism patterns 1 and 3. Number of specimens (N), means and standard deviations (X ± SD) are reported for each taxon. F-values and associated probability statements derived from ANOVA are given for comparisons within (WITHIN) and between (BETWEEN) prism pattern categories.

TAXON	N	X ± SD in μm	WITHIN	BETWEEN
PRISM PATTERN 1				
Atelerix albiventris	3	2.51 ± .098		
Erinaceus europaeus	2	2.44 ± .361	F = 3.648 n.s.	
Tupaia glis	3	1.88 ± .730		
				F = 11.400 p < .01
PRISM PATTERN 3				
Balantiopteryx plicata	4	2.86 ± .895		
Rhinopoma hardwickei	2	2.88 ± .828		
Taphozous mauritianus	2	3.40 ± .286		
Cynocephalus sp.	4	3.06 ± .667	F = 1.181 n.s.	
Homo sapiens	5	3.71 ± .349		
Microsyops sp.†	2	3.21 ± 1.29		
OTHER SAMPLED TAXA				
Cercocebus albigena	2	4.83 ± .968		
Cercocebus torquatus	3	5.21 ± .525		
Macaca fasicularis	3	3.15 ± .418		
Galagoides alleni	1	4.98 ± 1.106		
Galagoides demidovii	1	6.16 ± .830		
Notharctus sp.†	1	2.39 ± .362		

† = fossil taxon; n.s.: not significant.

junction and the outer enamel surface of most mammalian teeth and is typically underlain and overlain, respectively, by a layer of pattern 1 enamel. These layers were formed as ameloblasts began and ended their enamel-secreting cycles (Boyde, 1964; Ripa *et al.*, 1966; Gwinnett, 1967; Martin, 1983; Fortelius, 1985; Martin *et al.*, 1988). Variation in prism pattern beyond that already mentioned above is also common within single teeth (e.g., von Koenigswald, 1992; von Koenigswald and Clemens, 1992). However, several studies of primate enamel have demonstrated that prism patterns are relatively constant in mid-thickness enamel (e.g., Boyde and Martin, 1982, 1984a, 1984b; Martin *et al.*, 1988). This level of consistency in mid-thickness prism patterns is also characteristic of the non-primate taxa included in this analysis (Dumont, 1993).

Enamel deposition rates may be estimated in mature enamel by measuring prism cross striation repeat intervals. This prism striation has been interpreted as representing circadian variation in enamel deposition rate (e.g., Gysi, 1931; Schour and Poncher, 1939; Boyde, 1964, 1979, 1989; Boyde and Martin, 1982, 1984a; Shellis, 1984b; Bromage and Dean, 1985; Risnes, 1986; Beynon and Reid, 1987; Dean, 1987a, 1987b). Although studies by several workers have suggested that cross striations are artifactual (e.g., Osborn, 1971;

Table 3. Raw cross-striation repeat interval (C.S.R.I.), tooth area, mean ameloblast area and body mass data. Body mass data for sexually dimorphic species is reported as a mean of male and female values. Product-moment correlation coefficients (r) between (log) cross striation repeat interval and (log)(√2 estimated ameloblast area), (log)(√2 tooth area), and (log)(√3 body mass) and the sample size (N) for each comparison are provided. None of the coefficients differ significantly from 0.

Taxon	Mean C.S.R.I.	Tooth Area	Mean A.A.	Body Mass
Order Lipotyphla				
Atelerix albiventris	2.51	12.46	17.72	485 g[1]
Erinaceus europaeus	2.44	23.33	20.98	912.5 g[2]
Order Scandentia				
Tupaia glis	1.88	7.51	30.80	200 g[2]
Order Chiroptera				
Balantiopteryx plicata	2.86	1.10	21.44	7.5 g[3]
Rhinopoma hardwickei	2.88	1.64	25.50	11 g[1]
Taphozous mauritianus	3.40	2.53	26.42	22.5 g[1]
Order Dermoptera				
Cynocephalus variegatus	3.06	14.75	29.38	1,250 g[3]
Order Primates				
Cercocebus albigena	4.83	15.13	-	7,690 g[4]
Cercocebus torquatus	5.21	62.88	-	10,625 g[4]
Galagoides alleni	4.98	7.34	-	295 g[4]
Galagoides demidovii	6.16	10.63	28.30	60 g[2]
Homo sapiens	3.71	-	31.36[5]	60,000 g[2]
Macaca fasicularis	3.15	28.84	-	4,030 g[4]
Notharctus sp.†	2.39	12.01	34.11	-
Order incerta sedis				
Microsyops sp.†	3.21	11.90	39.94	-

(log) Cross Striation Repeat Interval Against	(log) (sqrt) Tooth Area	(log) (sqrt) A.A.	(log) (cbrt) Body Mass
	r = .30	r = .16	r = .23
	N = 14	N = 11	N = .13
	n.s.	n.s.	n.s.

† = fossil taxon; n.s.: not significant.

[1]Kingdon (1974); [2]Eisenberg (1981) [3]Walker (1975); [4]Fleagle (1988); [5]Fosse (1968b).

Weber and Glick, 1975; Warshawsky and Bai, 1983; Warshawshy *et al.*, 1984), Bromage (1991) has provided experimental evidence that cross striations indeed represent cyclical variation in enamel deposition. Similar studies have demonstrated that such rhythms also characterize dentine deposition and endochondral ossification (e.g., Yilmaz *et al.*, 1977; Simmons, 1974; Kawasaki *et al.*, 1980). This study assumes that prism cross striations are manifestations of a constant physiological rhythm. Provided that the periodicity is the same for all taxa, the length of the rhythm period is not relevant to this analysis.

Because cross striations are considered in part to be manifestations of variation in carbonate concentrations within fully mineralized enamel (Boyde, 1979; Boyde and Jones, 1983), BSE was selected as the most appropriate technique for observing prism cross striations morphology. Although contrast in BSE images of perfectly flat specimens that are oriented perpendicular to the electron beam indicated only variation in atomic number (Postek *et al.*, 1980), specimens used in this study were etched, and consequently exhibited some surface topography. Comparisons of secondary electron and BSE images of a subset of the specimens illustrated that contrast permitting visualization of the cross striations was primarily based on BSE signal.

Statistical comparisons of cross striation repeat intervals support the hypothesis that depositional rates differ significantly between prism pattern categories. Based on the data presented here, pattern 1 enamel is deposited significantly more slowly than is pattern 3 enamel. That is, within the same period of time, larger segments of pattern 3 enamel prisms are deposited by an ameloblast than along pattern 1 enamel prisms. These differences in depositional rates transcend ordinal boundaries and appear to point to a basic relationship between ameloblast activity and the structure of fully mineralized enamel.

In contrast to the first hypothesis, the data analyzed here failed to support the second hypothesis that higher-level taxa are characterized by taxon-specific cross striation repeat interval values. Among pattern 1 taxa, prism cross striation repeat intervals do not differ significantly between erinaceids and scandentians. Similarly, there are no significant differences in cross striation repeat intervals among the four sampled pattern 3 taxa (*chiropterans*, *Homo sapiens*, *Microsyops* sp., and *Cynocephalus variegatus*). That diverse taxa exhibiting the same prism patterns are homogeneous with respect to deposition rate again supports the conclusion that prism pattern and depositional rate are closely associated.

Despite the suggestions of previous workers that enamel deposition rate is correlated with either body or ameloblast size (Boyde, 1969; Martin, 1983), no evidence for these assertions was found within the data presented here. Based on these data, deposition rates are not correlated with either tooth area, body mass, or estimated ameloblast area. By inference, these data also suggest that prism pattern is not correlated with any of these factors.

The association between prism pattern and cross striation repeat intervals obtained in this study are in general accord with those reported by other workers. Intervals for pattern 1 enamel have been reported in most instances to remain below 2.5 μm (Martin, 1983; Boyde and Martin, 1984; but see Shellis and Poole, 1977). This is supported by the species means for pattern 1 taxa within this study which range from 1.88 μm to 2.51 μm. Cross striation repeat interval values for pattern 3 enamel have been reported to range between 2 μm and 7 μm (Shellis and Poole, 1977; Martin, 1983; Martin and Boyde, 1984; Risnes, 1986). Although the mean cross striation repeat intervals reported here for pattern 3 enamel are on the low end of the reported range, they are nonetheless significantly higher than those found to characterize pattern 1 cross striation repeat intervals. In sum, the data presented here support the consensus opinion that pattern 1 cross striation repeat intervals are much smaller than those for pattern 3.

The length of cross striation repeat intervals for the cercopithecids are most similar to those of the pattern 3 species, though they are significantly larger ($p < .03$). While cercopithecid prism patterns exhibit a large proportion of pattern 2 spatial distribution, they do not exhibit the clearly defined inter-row sheets that are characteristic of pattern 2 enamel. The degree of variability in the spatial distribution of cross-sectioned prisms also makes it difficult to assign these taxa to prism pattern 3. These data suggest that slightly modified definitions of prism patterns may more accurately reflect the variability in the spatial distribution of arc-shaped prisms that is encountered as more mammalian species are sampled. For example, the consistent presence of vertically oriented inter-row sheets could be the determining factor in categorizing an enamel as pattern 2 while prisms pattern 3 could encompass all other spatial distributions of arc-shaped prisms.

The single specimens representing *Galagoides demidovii* and *Notharctus* sp. exhibit pattern 3 prisms. Although prism pattern could not be resolved for *G. alleni*, it is likely that it too exhibits the pattern 3 enamel that characterizes its congener. The cross striation repeat intervals of the two galago species accord most closely with those of other pattern 3 taxa. In contrast, the mean cross striation repeat interval of Notharctus falls into the range of prism pattern one taxa. Nevertheless, it also lies within one standard deviation of other pattern 3 cross striation repeat interval means. Because the cross

striation repeat interval mean for *Notharctus* is based on a sample of only six cross-striations, it is likely that further study of *Notharctus* enamel will lead to a more reliable assessment of the range of cross striation repeat interval values for the species.

Summary and Conclusions

Prism patterns are significantly associated with enamel deposition rates. Therefore, fluctuations in rate among lower-level taxa may be associated with the heterogeneous prism patterns often seen at higher taxonomic levels. The immediate mechanism producing changes in deposition rate is unknown, although such changes could arise through the pleiotropic effects of alterations in any number of physiological systems.

Variation in prism patterns is common within orders and, to a lesser extent, within families (Boyde, 1964; Carlson and Krause, 1985; Skobe *et al.*, 1985; Martin *et al.*, 1988; von Koenigswald and Clemens, 1992; Dumont, 1993). Despite this variation, many family-level taxa can be characterized by a typical prism pattern. This conservation of prism pattern suggests that although prism patterns are associated with depositional rates, these rates and the factors controlling them do not vary extensively within families. It seems likely, therefore, that prism patterns are potentially reliable phylogenetic characters when they are applied below the ordinal level. However, recognizing the presence of variation in prism pattern within and between individuals, one must sample enamel prism patterns at homologous tooth positions and depths for several individuals from each taxon in order to accurately assess the predominant prism pattern of any taxonomic group.

Acknowledgements

I thank curators at the following institutions for the loan of specimens used in this study; Academy of Natural Sciences, Philadelphia (ANSP): Carnegie Museum (CM), Department of Anatomical Sciences - S.U.N.Y. at Stony Brook (SUSB), Department of Zoology - University of Michigan (DZUM), Florida Museum of Natural History (FMNH), Florida State Museum (FSM), Rijksmuseum Van Natuurlijke Historie (RVNH), and Texas Tech University Museum (TT). I also thank Dr. David Krause for comments regarding this manuscript and Drs. Lawrence Martin and Fred Grine for access to and assistance with scanning electron microscopy. This project was supported by an NSF dissertation improvement grant (BNS 8922966).

References

Beynon AD, Reid DJ (1987). Relationship between perikymata counts and crown formation times in the human dentition. J. Dent. Res. **66**: 889 (abstract).

Boyde A (1964). The structure and development of mammalian dental enamel. Unpublished Ph.D. Thesis, University of London.

Boyde A (1967). The development of enamel structure. Proc. R. Soc. Med. **60**: 1-6.

Boyde A (1969). Correlation of ameloblast size with enamel prism pattern: use of scanning eiectron microscope to make surface area measurements. Z. Zellforsch. Mikrosk. Anat. **93**: 583-593.

Boyde A (1971). Comparative histology of mammalian teeth. In: Dental Morphology and Evolution. Dahlberg A (ed.). University of Chicago Press, Chicago. pp. 81-94.

Boyde A (1979). Carbonate concentration, crystal centers, core dissolution, caries, cross striations, circadian rhythms and compositional contrast in SEM. J. Dent. Res. **58(B)**: 981-983.

Boyde A (1989). Enamel. In: Handbook of Microscopic Anatomy. Volume V/VI: Teeth. Oksche A, Vollrath L (eds.). Springer-Verlag, Berlin. pp. 309-373.

Boyde A, Jones SJ (1983). Backscattered electron imaging of dental tissues. Anat. Embryol. **168**: 211-226.

Boyde A, Martin LB (1982). Enamel microstructure determination in hominoid and cercopithecoid primates. Anat. Embryol. **165**: 193-212.

Boyde A, Martin LB (1984a). A non-destructive survey of prism packing patterns in primate enamels. In: Tooth Enamel IV. Fearnhead RW, Suga S (eds.). Elsevier Press, Amsterdam. pp. 417-426.

Boyde A, Martin LB (1984b). The microstructure of primate dental enamel. In: Food Acquisition and Processing in Primates. Chivers DJ, Wood BA, Bilsborough A (eds.). Plenum Press, New York. pp. 341-367.

Boyde A, Martin LB (1987). Tandem scanning microscopy of primate enamels. Scanning Microsc. **1**: 1935-1948.

Bromage TG (1991). Enamel incremental periodicity in the pig-tailed macaque: a polychrome fluorescent labeling study of dental hard tissues. Am. J. Phys. Anthropol. **86**: 205-214.

Bromage TG, Dean MC (1985). Re-evaluation of the age at death of immature fossil hominids. Nature **317**: 525-527.

Carlson SJ, Krause DW (1985). Enamel ultrastructure of multituberculate mammals: an investigation of variability. Contrib. Mus. Paleontol. Univ. Mich. **27(1)**: 1-50.

Dean MC (1987a). Growth layers and incremental markings in hard tissues: a review of literature and some

preliminary observations about enamel microstructure in *Paranthropus boisei*. J. Hum. Evol. **16**: 197-213.

Dean MC (1987b). The dental development status of six East African juvenile fossil hominids. J. Hum. Evol. **16**: 197-213.

Dumont ER (1993). Functional and phyletic features of mammalian dental enamel: implications for primates higher-level relationships. Ph.D. thesis, S.U.N.Y. at Stony Brook, Stony Brook, New York.

Eisenberg JF (1981). The Mammalian Radiations: An Analysis of Trends in Evolution, Adaptation, and Behavior. University of Chicago Press, Chicago. pp. 464-471.

Fleagle JG (1988). Primate Adaptation and Evolution. Academic Press, New York. pp. 95, 165, 168.

Fortelius M (1985). Ungulate cheek teeth: developmental, functional, and evolutionary implications. Acta Zool. Fenn. **180**: 1-76.

Fosse G (1968a). A quantitative analysis of the numerical density and the distributional pattern of prisms and ameloblasts in dental enamel and tooth germs. III. The calculation of prism diameters and the number of prisms per unit area in dental enamel. Acta Odontol. Scand. **26**: 315-336.

Fosse G (1968b). A quantitative analysis of the numerical density and the distributional pattern of prisms and ameloblasts in dental enamel and tooth germs. VIII. The numbers of cross-sectioned ameloblasts and prisms per unit area in tooth germs. Acta Odontol. Scand. **26**: 573-603.

Fosse G, Kielan-Jaworowska Z, Skaale SG (1985). The microstructure of tooth enamel in multituberculate mammals. Paleontology **28(3)**: 435-449.

Gantt DG (1982). Neogene hominoid evolution: a tooth's inside view. In: Teeth: Form, Function, and Evolution. Kurten B (ed.). Columbia University Press, New York. pp. 93-108.

Gantt DG (1983). The enamel of Neogene hominoids: structural and phyletic implications. In: New Interpretations of Ape and Human Ancestry. Ciochon RL, Corruccini RS (eds.). Plenum Press, New York. pp. 249-298.

Grine FE, Krause DW, Martin LB (1985). The ultrastructure of *Oreopithecus bramboli* tooth enamel: systematic implications. Am. J. Phys. Anthropol. **166**: 177-178 (abstract).

Grine FE, Krause DW, Jungers WL (1986). Analysis of enamel ultrastructure in archaeology: the identification of *Ovis aries* and Capra hircus dental remains. J. Archaeol. Sci. **13**: 579-595.

Grine FE, Krause DW, Fosse G, Jungers WL (1987). Analysis of individual, intraspecific and interspecific variability in quantitative parameters of caprine tooth enamel structure. Acta Odontol. Scand. **45**: 1-23.

Gwinnett AJ (1967). The structure of the "prismless" enamel of permanent human teeth. Arch. Oral Biol. **12**: 381-387.

Gysi A (1931). Metabolism in adult enamel. The Dental Digest **37**: 661-668.

Kawasaki K, Tanaka KS, Isikawa T (1980). On the daily incremental lines in human dentine. Arch. Oral Biol. **24**: 939-943.

Kingdon J (1974). East African Mammals, An Atlas of Evolution in Africa, Volume IIA, Insectivores and Bats. University of Chicago Press, Chicago. pp. 30, 206, 216.

Korvenkontio VA (1934-1935). Mikroskopische Untersuchungen an Nagerincisiven unter Hinweis auf die Schmelzstruktur der Backenzähne (Microscopic investigations on incisors with respect to the enamel structure of the teeth.) Ann. Zool. Soc. Zool.-Bot. Fennicae Vanamo **2**: 1-274.

Krause DW, Carlson SJ (1986). The enamel structure of multituberculate mammals: a review. Scanning Microsc. **4**: 1591-1607.

Lester KS, Hand SJ (1987). Chiropteran enamel structure. Scanning Microsc. **1**: 421-436.

Lester KS, Hand SJ, Vincent F (1988). Adult phyllostomid (bat) enamel by scanning electron microscopy - with a note on dermopteran enamel. Scanning Microsc. **2**: 371-383.

Martin LB (1983). The relationships of the later Miocene Hominoidea. Ph.D. thesis, University College, London.

Martin LB (1985). Significance of enamel thickness in hominoid evolution. Nature **314**: 260-263.

Martin LB, Boyde A (1984). Rates of enamel formation in relation to enamel thickness in hominoid primates. In: Tooth Enamel IV. Fearnhead RW, Suga S (eds.). Elsevier Press, Amsterdam. pp. 447-451.

Martin LB, Boyde A, Grine FE (1988). Enamel structure in primates: a review of scanning electron microscope studies. Scanning Microsc. **2**: 1503-1526.

Moss ML (1969). Evolution of mammalian dental enamel. Am. Mus. Novit. **2360**: 1-39.

Osborn JW (1970). The mechanism of prism formation in teeth: a hypothesis. Calcif. Tissue Res. **5**: 115-132.

Osborn JW (1971). A relationship between the brown striae of Retzius and prism directions in the transverse plane of the human tooth. Arch. Oral Biol. **16**: 1055-1060.

Postek MT, Howard KS, Johnson AH, McMichael KL (1980). Scanning Electron Microscopy: A Student's Handbook. Ladd Research Industries, Inc.

Ripa LW, Gwinnet AJ, Bunocore MG (1966). The "prismless" outer layer of deciduous and permanent

teeth. Arch. Oral Biol. **11**: 41-48.

Risnes S (1986). Enamel apposition rate and the prism periodicity in human teeth. Scand. J. Dent. Res. **94**: 394-404.

Schour I, Poncher HC (1939). The rate of apposition of human enamel and dentine as measured by the effects of acute fluorosis. Am. J. Dis. Child. **54**: 757-776.

Shellis RP (1984a). Inter-relationships between growth and structure of enamel. In: Tooth Enamel IV. Fearnhead RW, Suga S (eds.). Elsevier Press, Amsterdam. pp. 467-471.

Shellis RP (1984b). Variations in growth of the enamel crown in human teeth and a possible relationship between growth and structure. Arch. Oral Biol. **29**: 697-705.

Shellis RP, Poole DFG (1977). The calcified dental tissues of primates. In: Evolutionary Changes to the Primate Skull and Dentition. Lavelle LLB, Shellis RP, Poole DFG (eds.). Thomas Company, Springfield, Illinois. pp. 197-279.

Silness J, Gustavsen F (1969). Structure of the organic matrix of dental enamel in the hedgehog (*Erinaceus europaeus*). Odontol. Revy **20** (sup. 19): 1-41.

Simmons DJ (1974) Chronobiology of endochondral ossification. Chronobiol. **1**: 97-109.

Skobe Z, Proztak KS, Trombly PL (1985). Scanning electron microscope study of cat and dog enamel structure. J. Morphol. **184**: 195-204.

Smith RJ (1984). Allometric scaling in comparative biology: problems of concept and method. Am. J. Phys. Anthropol. **246**: 152-160.

Sokal RR, Rohlf FJ (1981). Biometry, the Principles and Practice of Statistics in Biological Research. W.H. Freeman and Company, New York.

von Koenigswald, W (1992). Tooth enamel of the cave bear (*Ursus spelaeus*) and the relationship between diet and enamel structure. In: Memorial volume Bjorn Kurten (Forsten A, Fortelius M, Werdelin L, eds.), Annales Zool. Fennica **28**: 217-227.

von Koenigswald W, Clemens WA (1992). Levels of complexity in the microstructure of mammalian enamel and their application to studies of systematics. Scanning Microsc. **6**: 195-217.

Walker EP (1975). Mammals of the World. Johns Hopkins University Press, Baltimore, MD. pp. 180, 240.

Warshawsky H, Bai P (1983). Knife chatter during thin sectioning of rat incisor enamel can cause periodicities resembling cross-striations. Anat. Rec. **207**: 533-538.

Warshawsky H, Bai P, Nanci A (1984). Lack of evidence for rhythmicity in enamel development. Colloques de l'Institut National de la Santé et de la Recherche Médical (INSERM) **125**: 241-256.

Weber DF, Glick PL (1975). Correlative microscopy of enamel prism orientation. Am. J. Anat. **144**: 407-420.

Yilmaz S, Newman HN, Poole DFG (1977). Diurnal periodicity of von Ebner growth lines in pig dentine. Arch. Oral Biol. **22**: 511-513.

Discussion with Reviewers

S. Risnes: In the paper, it is suggested that the prism pattern is dependent on the rate of enamel production. Is it not possible that the opposite is the case, i.e., that the rate of enamel production is dependent on the prism pattern, i.e., on the spatial arrangement of the ameloblasts?

Author: I have attempted to refrain from confusing correlation with causation when discussing the relationship between the rate of enamel deposition and prism pattern. The data presented here do not address the causal relationship between these two variables. It is entirely possible that either the rate of enamel deposition or the spatial arrangements of ameloblasts is the factor that drives the relationship between the two. It is also possible that these factors are not causally related but that prism pattern and deposition rate are both mediated by other, yet undocumented, variables.

S. Risnes: The term "enamel deposition rate" is ambiguous until the direction of the incremental growth is defined. Generally, this term means the growth in thickness of the enamel layer along a direction perpendicular to the incremental lines (Retzius lines). Since enamel prisms often deviate from such a direction, the rate of enamel deposition along the direction of the prisms will have to be higher than the rate of enamel deposition along a direction perpendicular to the incremental lines. To what extent will a distinction between these two rates affect your interpretations and discussion?

Author: In this study, "enamel deposition rate" was considered to be the rate of enamel accretion along individual prism long axes. The relationship of this rate of enamel deposition was not studied relative to larger incremental features (i.e., Retzius lines). Clearly, the data presented here do not directly address the issue of incremental growth as defined by an increase in enamel thickness. For the reasons that you cite, the distinction between prism accretion rate and the rate of increase in enamel thickness is critical for structurally complex enamels. However, most of the taxa included in this study do not exhibit prism decussation and, because of the relatively simple course taken by the prisms, it is possible that the rates of prism deposition reported here are, at least in part, reflective of the rate of enamel

increase. Certainly, a detailed assessment of the relationship between the two rates is required before definitive statements can be made.

W.A. Clemens: In your analysis of cross striation repeat intervals, you make use of mean values for specimens. Did you detect any repeated patterns in variation in the length of interval related to the area of the tooth (cusp slope or trigonid basin) sampled?
Author: For the one instance in which data collected from the buccal aspect of the protoconid slope and the trigonid basin were combined to generate a species mean (*Galagoides alleni* CM3898), cross striae from within the trigonid basin were significantly smaller (3.92 ± 0.162 versus 5.92 ± 0.1; $p < .001$). Because this study was designed to focus on enamel sampled from the external aspect cusp slopes, this is the only individual for which this comparison can be made. This result is intriguing, however, since it suggests that separate functional surfaces may develop in different ways (at least in respect to enamel deposition rates).

W.A. Clemens: Did you detect any correlation between thickness of mature enamel and prism type? Were thicker enamels usually characterized by the presence of pattern 3 prisms?
Author: Enamel thickness data for several species of known enamel prism type are available (Dumont, in press). Species that exhibit pattern 3 prisms exhibit on average slightly higher relative enamel thickness values (6.44 ± 1.76, $N = 7$) than do species that exhibit pattern 1 prisms (5.0 ± 0.57, $N = 2$). However, these values are not significantly different ($p = 0.31$). Clearly, these sample sizes are quite small and additional data is required to accurately assess the relationship between prism pattern and enamel thickness.

M.A. Saunder: If prism pattern and deposition rate are correlated, could prism patterns be a by-product of different prism deposition rates necessary to form certain enamel types? For example, maybe Hunter-Schreger Bands require faster deposition than radial enamel. In an enamel organ depositing both enamel types at the same time (as is commonly the case), two different prism patterns in the same enamel would be the necessary result. This could be an explanation of the limited phylogenetic information content of prism patterns.
Author: It is entirely possible that variation in prism patterns is associated with variation in deposition rates needed to form different types of enamel. This is a very interesting hypothesis in that it proposes a functional requirement as the driving force for variation enamel deposition rates. I would venture that further investigation along these lines would provide some interesting results.

Additional Reference

Dumont ER. Enamel thickness and dietary adaptation among extant primates and chiropterans. J. Mammal (in press).